

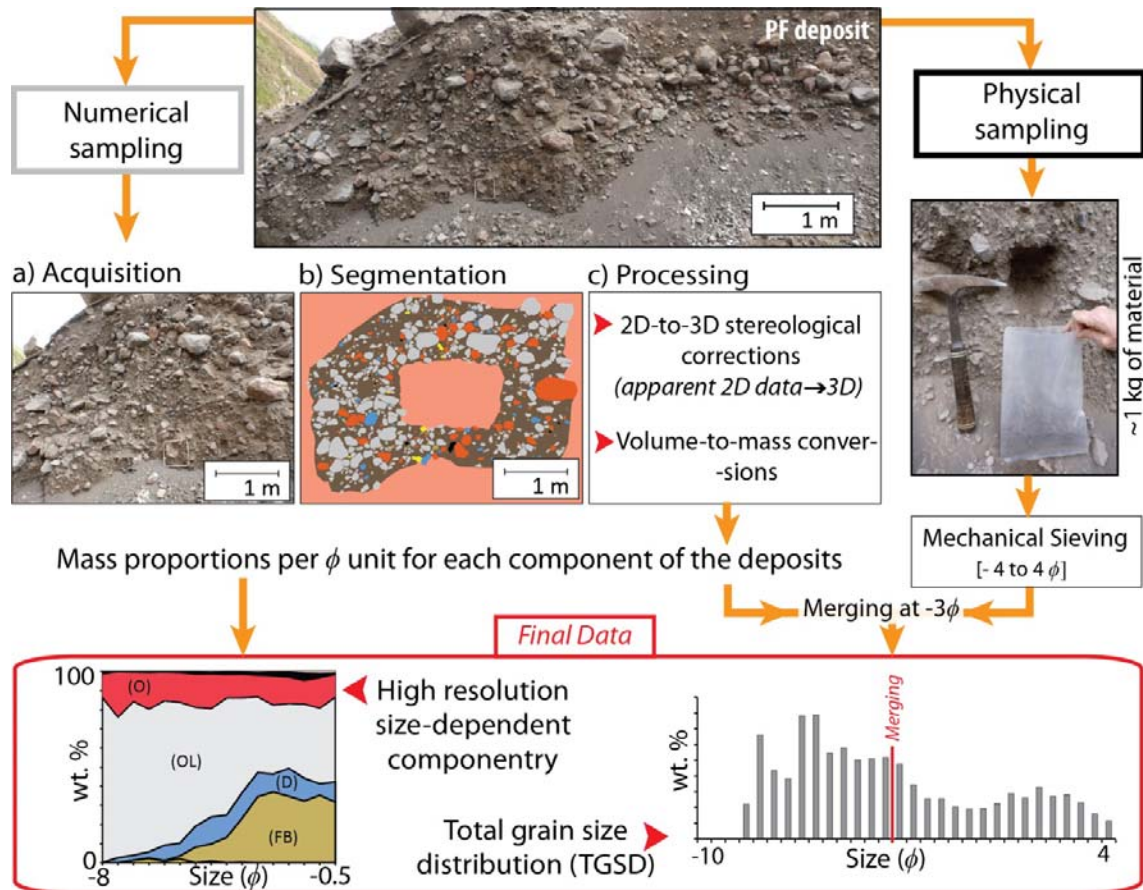
**Electronic supplementary material related to the article “The milling
factory: componentry-dependent fragmentation and fines production in
pyroclastic flows” by J. Bernard and J.-L. Le Pennec**

We investigated 26 clean exposures of PF deposits, including 18 at the base of the volcano and 8 along the Northwestern “Juive Grande” ravine from 2200 m to 3300 m a.s.l. (see Fig. 1 of the article). Our method to describe PFs deposits grain size distribution and componentry over a large grain size array is based on the twin analysis of digital images and physical samples of the products, respectively. The first method focuses on the coarse size range whereas the second one concentrates on the lapilli and ash size range. A “numerical digital sample” is formed by a set of high resolution images taken at right angle to the outcrop surface, using several magnifications to capture the largest size range (see Fig. 1 of the ESM and Bernard et al., 2014). Relevant textural features (shape, color, aspect, etc.) of each lithological componentry class were determined in the field to set up an impartial determination key to unambiguously distinguish them. Manual on-screen segmentation of individual clasts (apparent 2D-projected outline) of digital numerical samples using under Photoshop© software lead to the identification of large populations of clasts (1,000 to 3,400 per sample). Size, number and lithology of segmented clasts are used to determine 2D grain size distribution (GSD) and componentry proportions of the coarse-grained fraction of the deposits. To convert our apparent 2D data into 3D clast populations, we used the stereological unfolding method correcting the probability of intersection and cross-section effect inherent to 2D data (Sahagian and Prousevitch, 1998; Shea et al., 2010; Jutzeler et al., 2012). The resulting volume data are then converted into masses using clast specific densities measured by Eychenne et al. (2012) on the same 2006 products (Bernard et al., 2014). ~60,000 clasts were manually on-screen-segmented during image analysis and pigeonholed in the seven identified lithological classes.

Granular matrix samples consist of ~1 kg of lapilli-sized to fine-grained material carved across a ~10 x 10 cm square surface inside the matrix on subvertical exposure (Fig. 1). Grain-size measurements were performed in the laboratory by dry sieving between -4 and 4 ϕ (16 mm – 63 μ m, respectively). Grain-size distribution curves (GSD) were reconstructed by combining the data retrieved from the digital approach (below -3 ϕ) with those obtained from mechanical sieving (above -3 ϕ) image- and sieving-derived data at the cutting value of -3 ϕ .

32 The lithological composition (i.e. the componentry) of the matrix fractions was determined on
 33 selected samples and grain-size range by particle hand-picked counting under magnifying
 34 binocular (at least 300 grain per size range, following Eychenne et al., 2013).

35 The apparent 2D morphology of each image-segmented clast is reported as circularity ($C_c =$
 36 $(4\pi A)/P^2$) and convexity ($C_v = P_{CH}/P$), where A is the apparent (2D) particle area, P is the
 37 apparent perimeter and P_{CH} is the perimeter of the convex hull (Leibbrandt and Le Pennec,
 38 2015).



39

40 **Fig. 1:** Summary of the different methodological steps allowing reconstructing high-resolution side-
 41 dependent componentry and grain size distribution (GSD) of PF samples by combining numerical
 42 image-based and physical sampling. See ESM text for further explanations on each step.

43 REFERENCES

44 Bernard, J., Kelfoun, K., Le Pennec, J.-L., and Vallejo Vargas, S., 2014, Pyroclastic flow
 45 erosion and bulking processes: comparing field-based vs. modeling results at
 46 Tungurahua volcano, Ecuador: Bulletin of Volcanology, v. 76, p. 1-16,
 47 doi:10.1007/s00445-014-0858-y.

- 48 Eychenne, J., Le Pennec, J.-L., Troncoso, L., Gouhier, M., and Nedelec, J.-M., 2012, Causes
49 and consequences of bimodal grain-size distribution of tephra fall deposited during the
50 August 2006 Tungurahua eruption (Ecuador): *Bulletin of Volcanology*, v. 74, p. 187-
51 205, doi:10.1007/s00445-011-0517-5.
- 52 Eychenne, J., Le Pennec, J.-L., Ramón, P., and Yepes, H., 2013, Dynamics of explosive
53 paroxysms at open-vent andesitic systems: High-resolution mass distribution analyses
54 of the 2006 Tungurahua fall deposit (Ecuador): *Earth and Planetary Science Letters*, v.
55 361, p. 343-355, doi:10.1016/j.epsl.2012.11.002.
- 56 Jutzeler, M., Proussevitch, A.A., and Allen, S.R., 2012, Grain-size distribution of
57 volcaniclastic rocks 1: A new technique based on functional stereology: *Journal of*
58 *Volcanology and Geothermal Research*, v. 239-240, p. 1-11,
59 doi:10.1016/j.jvolgeores.2012.05.013.
- 60 Sahagian, D.L., and Proussevitch, A.A., 1998, 3D particle size distributions from 2D
61 observations: stereology for natural applications: *Journal of Volcanology and*
62 *Geothermal Research*, v. 84, p. 173-196, doi:10.1016/S0377-0273(98)00043-2.
- 63 Shea, T., Houghton, B.F., Gurioli, L., Cashman, K.V., Hammer, J.E., and Hobden, B.J., 2010,
64 Textural studies of vesicles in volcanic rocks: An integrated methodology: *Journal of*
65 *Volcanology and Geothermal Research*, v. 190, p. 271-289,
66 doi:10.1016/j.jvolgeores.2009.12.003.